Macroscopic-Scale Template Synthesis of Robust Carbonaceous Nanofiber Hydrogels and Aerogels and Their Applications

6 AUTHORS, INCLUDING:

Chen Li-feng

University of Science and Technology of Ch…

12 PUBLICATIONS **734** CITATIONS

Shu-Hong Yu

University of Science and Technology of Ch…

367 PUBLICATIONS **15,314** CITATIONS

Nanofiber Gels

Macroscopic-Scale Template Synthesis of Robust Carbonaceous Nanofiber Hydrogels and Aerogels and Their Applications**

*Hai-Wei Liang, Qing-Fang Guan, Li-Feng Chen, Zhu Zhu, Wen-Jun Zhang, and Shu-Hong Yu**

Hydrogels and aerogels are two typical families of gels, classified according to the medium they encompass, that is, water and air, respectively. Hydrogels have not only pervaded our everyday life in a variety of forms (e.g., fruit jellies, toothpaste, contact lenses, and hair gel), but have also been extensively explored as functional soft materials for use in various scientific fields.[1,2] Replacing the liquid solvent in hydrogels or other wet gels by air without collapsing the network structure can lead to a new type of porous materials, namely, aerogels.[3,4] Particularly, 3D nanoscale networks with open pores in the gels allow access and fast diffusion of ions and molecules, and thus hydrogels/aerogels have exhibited excellent performance as super adsorbents,[5,6] electrode materials for batteries and supercapacitors,[7] catalyst supports,[8] and chemical and biological sensors.[9,10] Despite their outstanding potential, several challenges in aerogel synthesis still must be addressed prior to their extensive practical application. The major problem associated with conventional aerogels is poor mechanical stability. The mechanical strength of aerogels could be enhanced by nanocasting conformal polymer coatings on preformed 3D networks, but this was accompanied by dramatic decreases in their porosity.[11,12] Furthermore, to prevent the network from collapsing in a gel, supercritical drying is the most widely used technique for solvent removal. It is difficult to prepare low-cost aerogels on a large scale due to the limitations of industrial supercritical drying.

[*] Dr. H. W. Liang, Q. F. Guan, L. F. Chen, Z. Zhu, W. J. Zhang, Prof. S. H. Yu
Division of Nanomaterials and Chemistry, Hefei National Laboratory for Physical Sciences at Microscale, Department of Chemistry, National Synchrotron Radiation Laboratory, University of Science and Technology of China
Hefei, Anhui 230026 (China)
E-mail: shyu@ustc.edu.cn
Homepage: http://staff.ustc.edu.cn/~yulab/

Although several nanomaterials including carbon nanotubes,[13,14] cellulose nanofibers,[15] and the newly discovered graphene[16] have been recently used as building blocks and assembled into monolithic gels, there is a lack of precise control of their physicochemical properties, particularly the size of building blocks, the porosity, and their surface chemistry, which are crucial in the further design and functionalization of aerogels for various applications. Here we report a new class of monolithic hydrogels/aerogels consisting of highly uniform carbonaceous nanofibers (CNFs), based on the recent, well-developed template-directed hydrothermal carbonization (HTC) process.[17–19] Compared with the conventional process for aerogel preparation, our synthetic method has some significant advantages: 1) Direct scaleup from 30 mL to 12 L just by using a large autoclave and without changing reactant concentrations and reaction time; 2) Easy and precise control of the structural parameters and mechanical strength of the CNF hydrogels/aerogels over a wide range; and 3) Extraordinary flexibility and high chemical reactivity of the CNF gels give them great application potential.

The synthesis of CNF gels is illustrated in Figure 1a. Ultrathin Te nanowire (TeNWs)[20] templates are first dispersed in glucose solution to form a homogenous mixture (step 1 in Figure 1a). Hydrothermal treatment of the mixture at 180°C for 12–48 h results in a mechanically robust monolithic gel-like product, which occupies the whole Teflon container and can be taken out directly without any damage (step 2 in Figure 1a; see also Supporting Information Figure S1a). The as-prepared wet gel can be easily cut into the desired shape (Supporting Information Figure S1b). After washing and chemical etching to remove TeNWs (Supporting Information Figure S2), the CNF hydrogel is formed (step 3 in Figure 1a). To obtain the CNF aerogel, water in the hydrogel is removed by freeze-drying (step 4 in Figure 1a and Supporting Information Figure S1c). A low-magnification SEM image of the aerogel reveals a highly porous network structure consisting of disordered nanofibers with uniform size (Figure 1c, left). There is no apparent difference in CNF size and distribution over the whole monolithic gel (Supporting Information Figure S3), that is, the network structure is homogeneous. Further SEM observations indicate that these highly uniform nanofibers interconnect with each other to a high degree through numerous junctions (Figure 1c, right). We hypothesize that these junctions are responsible for the outstanding mechanical properties of the gels. Formation of junctions between CNFs is not difficult to understand. In the original mixture before hydrothermal treatment, it was unavoidable that the TeNWs physically contacted or approached each other if their concentration reached a critical
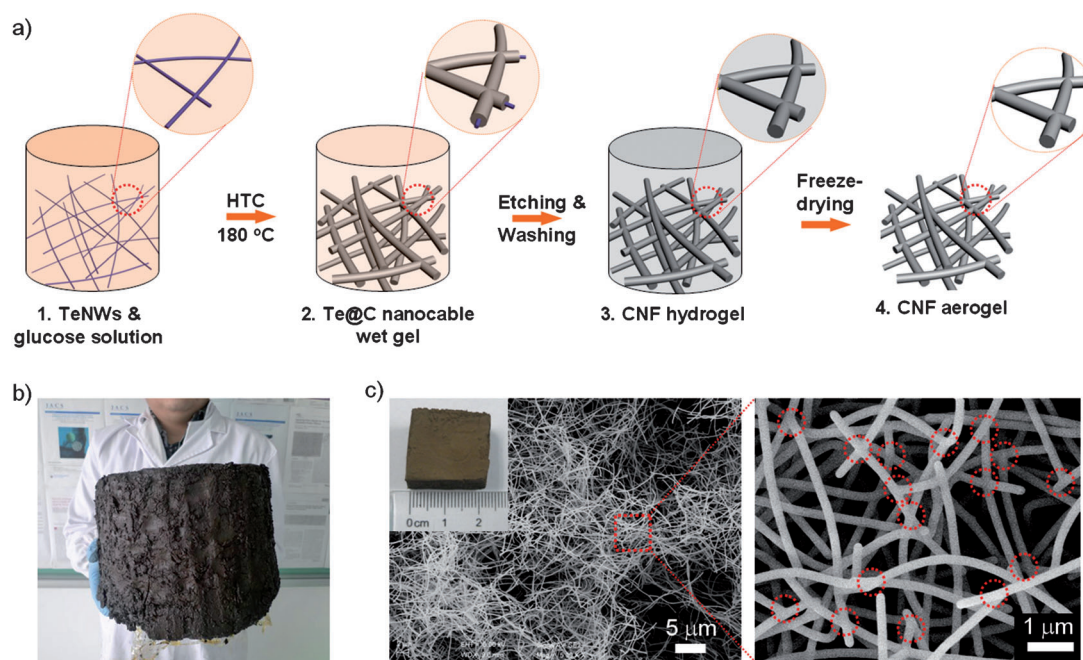
Figure 1. Large-scale fabrication of CNF hydrogels and aerogels. a) Schematic illustration of the synthetic steps. 1) Ultrathin TeNW templates were dispersed in a glucose solution. 2) Hydrothermal treatment of the mixture at 180°C created a monolithic wet gel consisting Te@C nanocables. 3) CNF hydrogel obtained after etching off the Te templates and washing. 4) CNF aerogel obtained after freeze-drying of the hydrogel. b) Photograph of an approximately 12 L monolithic wet gel, which was prepared by hydrothermal carbonization of 12 L of solution containing 800 g glucose and 16 mmol TeNWs for 18 h. c) SEM images of the CNF aerogel with different magnifications showing the nanowire network structure. The inset in the right image of c) shows a photograph of a CNF aerogel obtained after freeze-drying. The red circles in the left image of c) indicate the junctions between fibers.

value (Figure 1 a). When the HTC reaction began, the glucose molecules were dehydrated, polymerized, and finally formed the carbonaceous matrix, which conformally coated the TeNWs and "soldered" them together at the contact points (Figure 1 a and Supporting Information Figure S4). We could not prepare mechanically stable gel monoliths when the concentration of TeNWs was below 0.4 mM because too few junctions formed during the HTC process to generate a stable framework in the dilute TeNW solution. The as-prepared CNFs aerogels exhibit a relatively low BET surface area of 10–30 $m^2 g^{-1}$, depending on the diameters of the CNFs. The BET surface area increases to greater than 300 $m^2 g^{-1}$ after post-carbonization at high temperature, due to the formation of abundant micropores in the carbon matrix (Supporting Information Figure S5).

One of the unique advantages of the present method is its great versatility in scaling up the synthesis and controlling the microstructure and physical properties of CNF gels. The synthesis of both TeNW templates and subsequent CNF gels can be directly scaled up just by using a large autoclave (Supporting Information Figure S6). For example, we prepared a large CNF monolithic gel with a volume of 12 L by using a 16 L autoclave (Figure 1 b). It is quite possible to realize larger scale synthesis for industrial production by further enlarging the equipment. As far as we know, it is difficult to achieve such large-scale synthesis with conventional chemical vapor deposition (CVD) equipment.[6,21,22] In addition, the versatility of the synthesis also allows us to prepare a series of CNF gels with various CNF diameters,

porosities, and mechanical strengths by regulating the synthetic parameters (Supporting Information Table S1 and Figure S7). These CNF gels are referred to as CNF-*x*-*y*, where *x* and *y* are the amount of TeNWs in millimoles and HTC time in hours, respectively. The diameter of CNFs is highly dependent on both TeNW concentration and HTC time and can be precisely controlled in the range of tens to hundreds of nanometers (Supporting Information Table S1 and Figure S8). All of the CNF aerogel samples are extremely light (Supporting Information Table S1). The density of the lightest CNF aerogel with stable structure we have prepared is only 3.3 $mg cm^{-3}$ (CNF-0.8-12), and almost belongs to the lowest among reported values.[3] We believe that the large-scale synthesis, combined with the simplicity of freeze-drying, can significantly increase the feasibility of future industrial preparation and applications.

Another unique property of the CNF gels is their extraordinary flexibility, which allows for large deformations without fracture. In dramatic contrast to the brittle nature of traditional silica-based aerogels, the CNF gels can bear a compression strain as high as 80% and almost recover their original volume after release of the compression (Figure 2 a and Supporting Information Movie S1). Figure 2 b shows plots of compressive stress–strain (σ_{gel} versus ε) for the CNF-0.8-18 hydrogel at set ε maxima of 40, 60, and 80%. Two distinct stages were observed during the loading process: a linear-elastic region at $\varepsilon < 50\%$ followed by a densification region. The unloading curves show that the stresses remain above zero until $\varepsilon = 0$, and this suggests rapid and almost
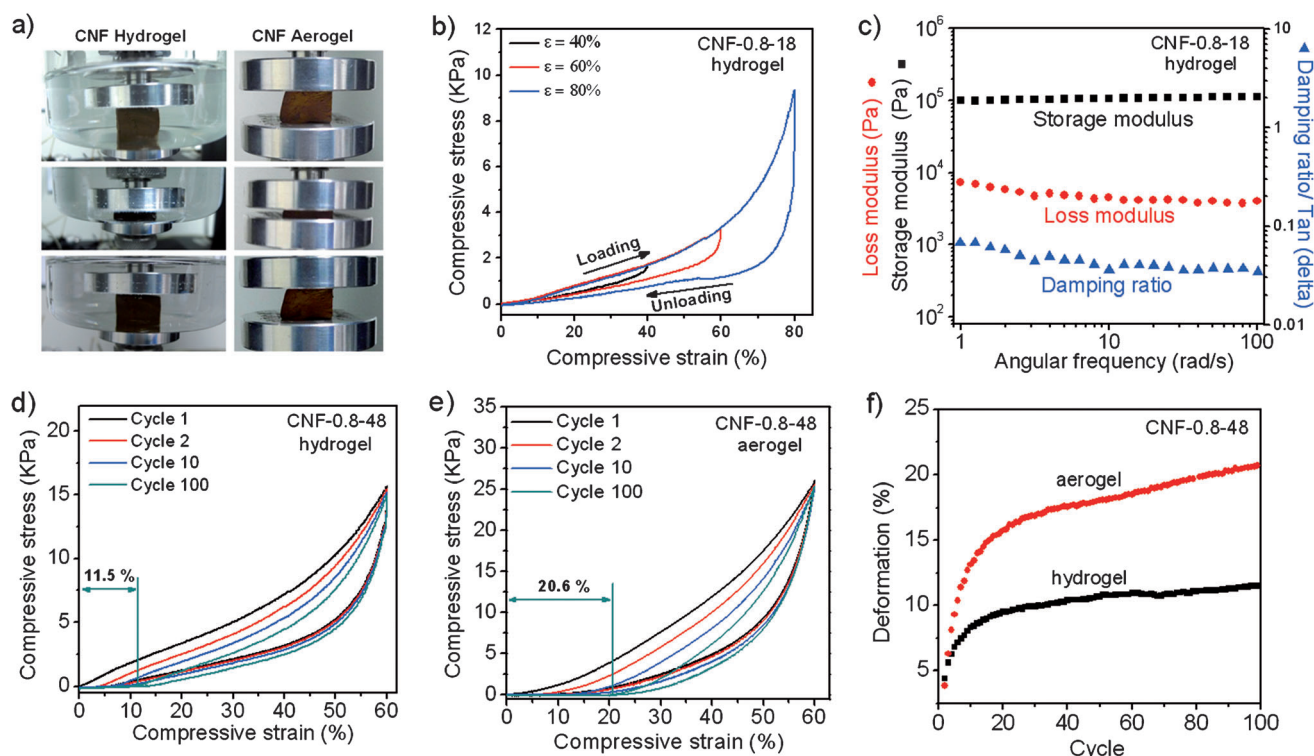
Figure 2. Mechanical properties of CNF hydrogels and aerogels. a) Sequential photographs of the CNF hydrogel (left) and aerogel (right) during the compression process, illustrating their robust mechanical properties. The hydrogel and aerogel were compressed in water and air, respectively. b) Compressive stress–strain (σ_{gel} versus ε) curves of CNF-0.8-18 hydrogel at different set strains ε of 40, 60, and 80%. c) Dynamic rheological behavior of CNF-0.8-18 hydrogel. Cyclic stress–strain curves of CNF-0.8-48 hydrogel (d) and aerogel (e) at a maximum strain of 60%, showing a permanent deformation of 11.5% (hydrogel) and 20.6% (aerogel) after 100 compression cycles. f) Deformation of CNF-0.8-48 due to compression for 100 cycles at a set strain of 60%.

complete recovery of the highly compressed CNF gels, in good agreement with the experimental observation (Figure 2 a). The CNF aerogels have similar compressive behavior to hydrogels, but exhibit higher compressive strength (Supporting Information Table S1 and Figure S9). The maximal stress (at $\varepsilon = 60\%$) of CNF-0.8-18 hydrogel and aerogel were measured to be about 12.1 and 28.3 kPa, respectively, that is, the CNF gel is a relatively soft material.[21] Prolonging the HTC time resulted in increased fiber size and solid content in the gels, which led to an obvious increase in their mechanical strength (Supporting Information Table S1 and Figure S10). Dynamic viscoelastic measurements were performed to further characterize the structure and properties of CNF hydrogels. The storage modulus G' of the gels is one order of magnitude higher than their loss modulus G''. A damping ratio of less than 0.1 over the entire tested range of angular frequencies (0.01–100 rad s^{-1}, Figure 2 c and Supporting Information Table S1) implies that elastic response is predominant and the gels have a strong and rigid network.

The CNF gels were subjected to a fatigue cyclic compression test ($\varepsilon = 60\%$) with 100 loading/unloading cycles (Figure 2 d and e). The maximum degradation in compressive strength of the CNF gels is less than 20% after 100 cycles. The thickness reduction after the fatigue test, indicated in Figure 2 d and e, is about 11.5 and 20.5% for hydrogel and aerogel, respectively. The plastic deformation of the aerogel is larger than that of hydrogel in the whole test process

(Figure 2 f), probably because the ice crystals formed during freeze-drying partly destroy the 3D network of the gels. No obvious structural changes were observed after the fatigue test (Supporting Information Figure S11). We attribute the robust mechanical properties of the CNF gels revealed by the fatigue tests to their unique interconnected 3D network, as illustrated schematically in Figure S12 of the Supporting Information.

Carbohydrates such as glucose can not be carbonized completely at a temperature as low as 160–200 °C. The process thus resulted in the formation of a large number of oxygen-containing groups on the carbonization products, especially hydroxyl and carboxyl groups. These functional groups endue the obtained carbonaceous materials not only with high adsorption capacity towards ionic pollutants but also with high chemical reactivity, which makes it easy to further decorate them with useful molecules or nanoparticles to form composites for various applications.[23,24] On the other hand, the interpenetrating, open-pore network characteristic of CNF gels permits rapid transport of gas- or liquid-phase molecular reactants and nanoscopic objects into, throughout, and out of the structure.[26] This ability makes the CNF gels ideal scaffolds around which to create novel composites. Here, on the basis of the high surface reactivity of the CNFs, the high porosity, and robust mechanical properties of gels, we demonstrate several potential applications of the CNF gels for the example of CNF-0.8-18.
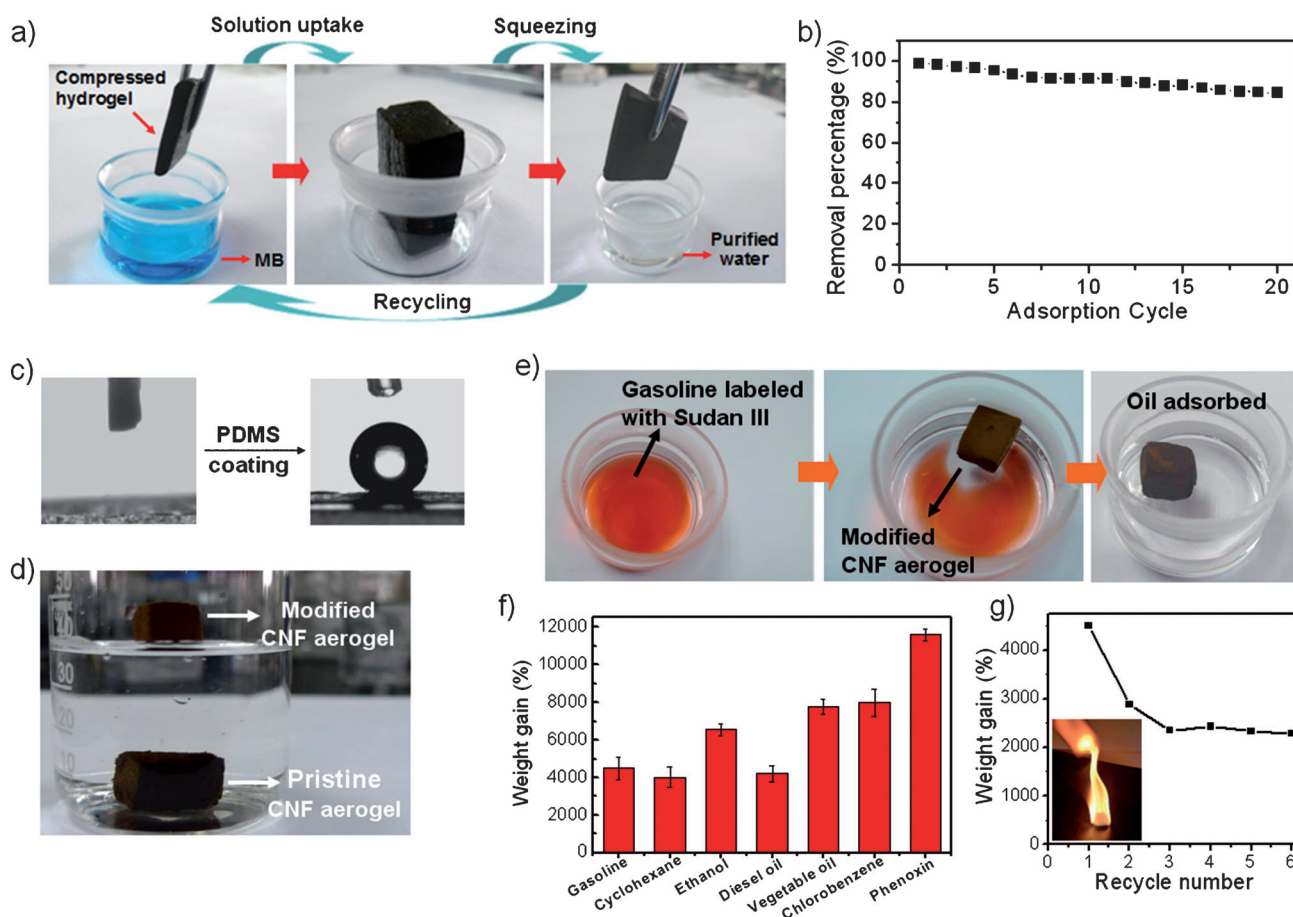
Figure 3. Controllable wetting behavior of the CNF aerogels and their selective adsorption properties. a) Photographs demonstrating facile removal of dye pollutant (MB), by exploiting the excellent adsorption performance of CNFs and the supercompressibility of the hydrogel. b) Removal percentage of MB as function of the number of uptake–squeezing cycles. c) Water contact angle measurements of the as-prepared CNFs aerogel (left) and silicone-coated aerogel (right). d) Photograph showing the controllable wetting behavior of the CNF aerogels towrds water. e) A layer of gasoline can be absorbed by the silicone-coated CNF aerogel. The gasoline was labeled with Sudan III for clarity. f) Absorption capacities of CNF aerogel for a range of organic solvents and oils in terms of weight gain. g) Regeneration capacity of the modified CNF aerogels for adsorption of gasoline. Gasoline can be directly burned from the aerogel for recycling. The inset shows a photograph of a burning aerogel saturated with gasoline.

The CNFs exhibit high adsorption rate and capacity for toxic metal ions and organic dyes.[26] The adsorption capacity of CNFs for methylene blue (MB) can be as high as about 800 mg g^{-1}. The combination of flexibility and excellent adsorption performance allow the CNFs hydrogels to be used directly as compressible adsorbents for simple removal of dye pollutants (Figure 3a and b). An as-prepared CNF hydrogel was first compressed into a compact sheet ($\varepsilon \approx 80\%$) to squeeze out most of its water content and then immerged in a 10 mg L^{-1} MB solution (left panel in Figure 3a). After uptake for only one minute, the CNF material was saturated with MB solution and had almost recovered its original shape (middle panel in Figure 3a). After standing for a further minute, the saturated CNF hydrogel was compressed again to squeeze out the decontaminated water, which appeared greatly decolorized compared with the original solution (right panel in Figure 3a, see also Supporting Information Movie S2). The degree of removal of MB was measured by UV/Vis spectroscopy to be as high as 98.5% (Supporting Information Figure S13). Moreover, the CNF hydrogel could

immediately be used in the next cycle and adsorbed 84.5% of MB even after 20 adsorption cycles (Figure 3b).

The CNF gels have further application potential as selective adsorbents for oil-spill cleanup (Figure 3c–g). To obtain superhydrophobic surfaces for selective uptake of oil, CNF-0.8-18 aerogel was coated with a conformal layer of polydimethylsiloxane (PDMS) to create a low-energy surface by employing a vapor deposition technique that allows the entire surface of the porous material to be coated. The PDMS-coated aerogel became superhydrophobic, as indicated by its high water-contact angle of $158 \pm 3°$. The modified aerogel floated on but did not absorb water, while the unmodified CNF aerogel was totally submerged (Figure 3d). Due to their surface superhydrophobicity and extra-high porosity (>99% for CNF-0.8-18), aerogels can easily remove oils or nonpolar organic solvents from water without adsorption of water, and this implies highly selective adsorption (Figure 3e). The aerogel showed uptake capacities up to 115 times its weight for a wide range of organic solvents and oils (Figure 3f), and thus this superhydrophobic aerogel is

a promising candidate as a suction skimmer in marine oil-spill recovery.[27] Importantly, the absorbed oil or solvents could be removed by direct combustion in air for recycled use (inset in Figure 3 g). After six adsorption/combustion cycles, a 23-fold weight gain ($>50\%$ of capacity in the first adsorption) was still achieved for gasoline (Figure 3 g).

Finally, the CNF gels can be employed as versatile 3D scaffolds to create composite gels. We first prepared CNF–Ag composite gels by in situ reduction of $AgNO_3$ (Supporting Information Figure S14). Micrographs showed that abundant AgNPs with a diameter of about 20 nm are uniformly distributed in the CNF matrix (Figure 4a and inset), and the
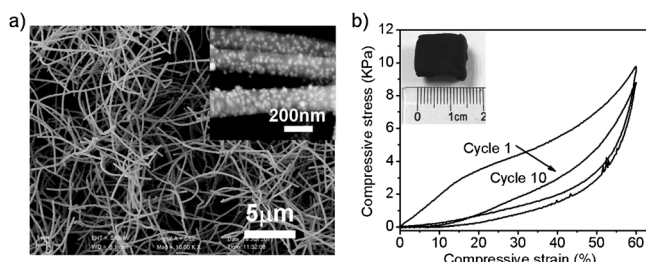

Figure 4. a) SEM image of the CNF–Ag aerogel. Inset: high-magnification image. b) Cyclic stress–strain curves of CNF–Ag aerogel at a set strain of 60%. Inset: photograph of the composite aerogel.

3D porous network of the gel was not destroyed after functionalization. Mechanical tests showed that the CNF–Ag composite aerogel exhibits similar compressibility to pure CNF aerogel (Figure 4b). Besides, fabrication of CNF–Pt and CNF–Au composite aerogels (see Supporting Information, particularly Figure S15) clearly demonstrates the versatility of the CNF gels as 3D scaffolds for creating functional composites.

In summary, we have demonstrated the fabrication of a new type of monolithic hydrogels/aerogels consisting of CNFs through a simple template-directed hydrothermal carbonization process. The CNF gels exhibit extraordinary compressibility, in marked contrast to the brittle nature of traditional low-density aerogels. The versatility of the present synthesis allows us to easily achieve large-scale synthesis (12 L) and control the diameter of the CNFs as well as the porosity and mechanical strength of the gels. By exploiting the high surface reactivity of the CNFs and extra-high porosity and robust mechanical properties of gels, we have demonstrated the great potential of gels for simple removal of dye pollutants, as selective adsorbents for oil-spill cleanup, and as versatile 3D templates for creating functional composite gels. Moreover, by post-carbonization treatment of the as-prepared CNF samples at high temperature, we can obtain highly conductive CNF aerogels with high surface area (Supporting Information Figure S16), which should find applications in a wide range of other fields, including conductive composites, catalyst supports, and 3D electrode materials for lithium-ion batteries and supercapacitors.

Experimental Section

Experimental details, characterization of the samples, SEM and TEM images, structural model, stress–strain curves, storage modulus and loss modulus of the CNF hydrogels as function of temperature, photographs of samples, and movies can be found in the Supporting Information.

[1] N. A. Peppas, Y. Huang, M. Torres-Lugo, J. H. Ward, J. Zhang, *Annu. Rev. Biomed. Eng.* **2000**, *2*, 9.
[2] N. M. Sangeetha, U. Maitra, *Chem. Soc. Rev.* **2005**, *34*, 821.
[3] N. Hüsing, U. Schubert, *Angew. Chem.* **1998**, *110*, 22; *Angew. Chem. Int. Ed.* **1998**, *37*, 23.
[4] A. C. Pierre, G. M. Pajonk, *Chem. Rev.* **2002**, *102*, 4243.
[5] K. Kabiri, H. Omidian, M. J. Zohuriaan-Mehr, S. Doroudiani, *Polym. Compos.* **2011**, *32*, 277.
[6] X. Gui, J. Wei, K. Wang, A. Cao, H. Zhu, Y. Jia, Q. Shu, D. Wu, *Adv. Mater.* **2010**, *22*, 617.
[7] D. R. Rolison, R. W. Long, J. C. Lytle, A. E. Fischer, C. P. Rhodes, T. M. McEvoy, M. E. Bourga, A. M. Lubers, *Chem. Soc. Rev.* **2009**, *38*, 226.
[8] C. Moreno-Castilla, F. J. Maldonado-Hodar, *Carbon* **2005**, *43*, 455.
[9] A. Richter, G. Paschew, S. Klatt, J. Lienig, K.-F. Arndt, H.-J. Adler, *Sensors* **2008**, *8*, 561.
[10] J. H. Zou, J. H. Liu, A. S. Karakoti, A. Kumar, D. Joung, Q. A. Li, S. I. Khondaker, S. Seal, L. Zhai, *ACS Nano* **2010**, *4*, 7293.
[11] N. Leventis, C. Sotiriou-Leventis, G. H. Zhang, A. M. M. Rawashdeh, *Nano Lett.* **2002**, *2*, 957.
[12] N. Leventis, *Acc. Chem. Res.* **2007**, *40*, 874.
[13] M. B. Bryning, D. E. Milkie, M. F. Islam, L. A. Hough, J. M. Kikkawa, A. G. Yodh, *Adv. Mater.* **2007**, *19*, 661.
[14] M. A. Worsley, S. O. Kucheyev, J. H. Satcher, A. V. Hamza, T. F. Baumann, *Appl. Phys. Lett.* **2009**, *94*, 073115.
[15] M. Pääkkö, J. Vapaavuori, R. Silvennoinen, H. Kosonen, M. Ankerfors, T. Lindstrom, L. A. Berglund, O. Ikkala, *Soft Matter* **2008**, *4*, 2492.
[16] Y. Xu, K. Sheng, C. Li, G. Shi, *ACS Nano* **2010**, *4*, 4324.
[17] B. Hu, K. Wang, L. H. Wu, S. H. Yu, M. Antonietti, M. M. Titirici, *Adv. Mater.* **2010**, *22*, 813.
[18] H. S. Qian, S. H. Yu, L. B. Luo, J. Y. Gong, L. F. Fei, X. M. Liu, *Chem. Mater.* **2006**, *18*, 2102.
[19] M. M. Titirici, M. Antonietti, *Chem. Soc. Rev.* **2010**, *39*, 103.
[20] H. S. Qian, S. H. Yu, J. Y. Gong, L. B. Luo, L. F. Fei, *Langmuir* **2006**, *22*, 3830.
[21] A. Y. Cao, P. L. Dickrell, W. G. Sawyer, M. N. Ghasemi-Nejhad, P. M. Ajayan, *Science* **2005**, *310*, 1307.
[22] M. Xu, D. N. Futaba, T. Yamada, M. Yumura, K. Hata, *Science* **2010**, *330*, 1364.
[23] H.-W. Liang, W.-J. Zhang, Y.-N. Ma, X. Cao, Q.-F. Guan, W.-P. Xu, S.-H. Yu, *Acs Nano* **2011**, *5*, 8148.
[24] P. Chen, H.-W. Liang, X.-H. Lv, H.-Z. Zhu, H.-B. Yao, S.-H. Yu, *Acs Nano* **2011**, *5*, 5928.
[25] D. R. Rolison, J. W. Long, *Acc. Chem. Res.* **2007**, *40*, 854.
[26] H.-W. Liang, X. Cao, W.-J. Zhang, H.-T. Lin, F. Zhou, L.-F. Chen, S.-H. Yu, *Adv. Funct. Mater.* **2011**, *21*, 3851.
[27] J. K. Yuan, X. G. Liu, O. Akbulut, J. Q. Hu, S. L. Suib, J. Kong, F. Stellacci, *Nat. Nanotechnol.* **2008**, *3*, 332.